Journal of Nuclear Materials 376 (2008) 336–340

Contents lists available at ScienceDirect

Journal of Nuclear Materials

journal homepage: www.elsevier.com/locate/jnucmat

Role of oxidation on LME of T91 steel studied by small punch test

T. Auger [a],*, I. Serre [b], G. Lorang [a], Z. Hamouche [a], D. Gorse [a], J.-B. Vogt [b]

[a] *CNRS, CECM, UPR2801, 15 rue Georges Urbain, 94407 Vitry sur Seine, France*
[b] *Laboratoire de Métallurgie Physique et Génie des Matériaux, ENSCL/USTL CNRS, Université de Lille 1, 59655 VILLENEUVE d'ASCQ cedex, France*

ARTICLE INFO

PACS:
61.25.Mv
61.14.Qp
62.20.Mk
68.49.Uv

ABSTRACT

A new technique for LME studies has been designed that makes use of the SPT coupled with a XPS/Auger spectroscopy analysis. The interface between the material (T91 steel) and the liquid metal (PbBi) can be varied to investigate the interplay between the oxide nature or the thickness and crack initiation induced by a liquid metal. It is shown in this work that LME can occur in some conditions on pre-oxidized surfaces indicating that there are other interfacial conditions than the oxide free intimate contact that could be detrimental to materials in contact with a liquid metal.

1. Introduction

Heavy liquid metals such as the lead bismuth eutectic (LBE) alloy are used or are envisioned to be used for heat transfer applications. Steels such as the austenitic AISI 316L or the martensitic T91 type, having good chemical compatibility with LBE, are the structural materials of choice for this medium. Liquid metal embrittlement (LME) is the transition from a ductile fracture mode to a brittle fracture one induced by a liquid metal under plastic deformation. LME of steels has therefore important technological implications. At the same time, this phenomenon is still poorly understood and the field did not grow in importance as much as stress-corrosion cracking. Most notable is the fact that very few detailed studies have been undertaken which make use of modern surface analysis in spite of the fact that it is well suited for such a phenomenon. This is quite surprising because LME is a surface induced effect controlled by the surface chemistry. This paper is a step forward to investigate the use of surface analysis techniques that could be useful in order to reach a better understanding of this phenomenon.

The experimental requirements to observe LME are twofold: wetting by the liquid metal, which is presently understood as intimate contact i.e. oxygen free interface, and the occurrence of plastic deformation. It has been shown that the T91 martensitic steel is subjected to LME by liquid PbBi alloys when the protective native oxide is removed in a tensile test [1]. In this work, mechanical testing was performed using a cylindrical tensile geometry. Samples were prepared with an oxide free interface between a deposit of PbBi and the steel. It can be obtained by ion beam etching of the native oxide followed by a PVD deposit of a PbBi coating under ultra high vacuum (UHV). The advantage of this technique is that the solid coating prevents re-oxidation during handling between the UHV chamber and the mechanical testing setup. Here, we present an improvement of the technique which uses the small punch test (SPT) coupled with Auger electron spectroscopy (AES) or X-ray photo-spectroscopy (XPS). SPT is a simple mechanical test that allows the investigation of crack initiation in a bi-axial stress state. One of the advantages of this test is that crack initiation proceeds near the surface making it quite sensible to any surface effect. Therefore, a change induced by the surface chemistry in the crack initiation process should be detected by this technique. Another advantage is that the required sample size is small. This testing geometry has been adapted recently to work with liquid metals by using flat discs of 8.9 mm diameter and of 500 μm thickness [2]. It opens up new possibilities for detailed investigation of the LME crack initiation mechanism because this is a perfectly suited size for applying surface analysis techniques such as Auger/XPS spectroscopy. Indeed, it has become customary for the last 30 years in corrosion science to study the oxide structure and evolution by Auger/XPS techniques [3,4]. Working under ultra high vacuum (UHV) also allows preparing surfaces with specific oxidation states. One can then test its impact on the crack initiation after a deposit of the liquid metal is performed in UHV. The crack initiation process under any liquid metal can then be studied for example as a function of the oxide layer thickness or composition.

In this work, the influence of the oxide on the protectiveness of the oxide layer has been investigated in the first oxidation stages using the SPT techniques described above. The importance of the surface state on the brittle or ductile crack initiation will be illustrated with the T91 martensitic steel in contact with PbBi. The goal

---

* Corresponding author. Tel.: +33 (0) 1 56 70 30 66; fax: +33 (0) 1 46 75 04 33.
E-mail address: auger@glvt-cnrs.fr (T. Auger).

0022-3115/$ - see front matter © 2008 Elsevier B.V. All rights reserved.
doi:10.1016/j.jnucmat.2008.02.076

is to have a better understanding of what constitutes a protective oxide 'vis-à-vis' LME.

2. Experimentals

Flat discs of 8.9 mm diameter and 500 μm thickness of T91 martensitic steel were machined from the as received alloy. The composition of the alloy is given in Table 1. The alloy is in the standard metallurgical state (austenitized at 1050 °C for 7 h, water quenched followed by a tempering heat treatment at 750 °C). The surface of the disc to be prepared under UHV was diamond polished down to 1 μm. The samples were taken to an Auger/XPS setup equipped with an ion gun and an Auger/XPS analysis setup. Before sputtering, the native oxide is composed of a mixture of external iron oxide and internal chromium oxide typical for a Fe–Cr alloy as can be seen on an Auger depth profile of a native oxide film on T91 (Fig. 1). The surface of the disc was ion beam etched with Krypton ions at an energy of 3 keV up to the disappearance of the O-KLL transition on Auger spectra (<1% monolayer surface coverage). After this cleaning step, four conditions have been investigated. The first one, labeled DNO2, is that of an oxygen free interface similar to the condition allowing LME in previous work [1]. In situ re-oxidation has also been performed according to two different conditions. At once, the clean samples were brought back after ion etching in the sample transfer chamber. The chamber was then filled by oxygen at 20 mbar pressure and the samples were re-oxidized during 0.5 h and from 4 to 8 h at the room temperature: they are labeled D0.5O2 and D4O2 respectively. Finally, in the fourth condition, the specimen was air oxidized in the transfer chamber at a 210 mbar O$_2$ pressure for 250 h (labeled DAO2). The sample transfer chamber was quickly vacuumed in order to transfer the samples into the UHV analysis chamber. Finally, the oxide thickness and the composition of the thin oxide film formed were characterized by XPS.

After the alloy surface has been re-oxidized and analytically characterized to a given level, a solid PbBi coating is deposited by physical vapor deposition (PVD). For that purpose, specimens in the condition DNO2, D0.5O2 and D4O2 were transferred a second time into the UHV sample transfer chamber to perform the PbBi coating. Those UHV conditions allow to prevent the sample surface from any composition modification before coating. A PbBi small ingot lying in a Ta basket was heated by the Joule effect to high temperature. The sample to be coated was brought in front of the basket so that evaporated PbBi could deposit on the prepared surface. After some exposure time (typically 5 min), the resulting thickness is of the order of 1 μm as it has been roughly estimated using SEM. As this deposit solidifies in UHV, it is enough to protect the interface from re-oxidation and to allow one to transfer in air without special care the sample to a SPT testing apparatus. Samples in the DAO2 condition were also coated by PVD after having been re-introduced in the UHV setup.

Table 1
Chemical composition of the T91 steel

Element	Cr	Mo	V	Mn	Si	Ni	C	Nb	Fe
Weight%	8.26	0.95	0.2	0.38	0.43	0.13	0.105	0.08	Balance

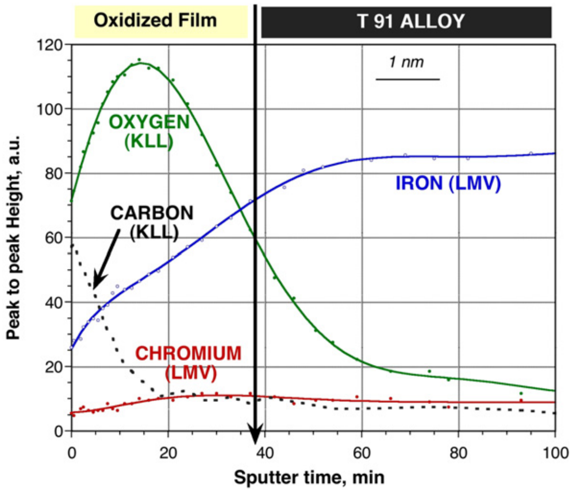

Fig. 1. AES depth profiles in a T91 steel native oxide film.

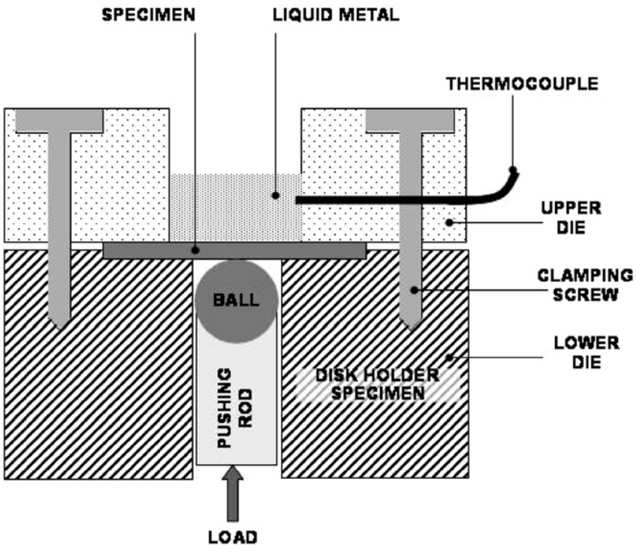

Fig. 2. Schematic of the small punch test set up.

The sample is then put in position in the SPT apparatus and fixed to the housing. The puncher ball made of tungsten carbide has a diameter of 2.5 mm (see Fig. 2). A heat ring surrounding the setup with the coated specimen is used to reach the test temperature within 15 min. The temperature is measured by a thermocouple located just above the sample. Experiments have been carried out at 250 °C and 300 °C. Immediately after reaching the desired temperature, the SPT were performed and the load-cross head displacement recorded. Punching has been stopped at the point where mechanical loading had dropped by 10%. Such a drop is indicative of the critical propagation of a large crack and it triggers the end of testing. Total testing duration did not exceed 15 min as well.

3. Analysis of the re-oxidized surface

The four conditions investigated in this work are given in Table 2.

X-ray photoelectron spectroscopy analysis of the re-oxidized surfaces were achieved with a MAC II CAMECA spectrometer (resolution $\Delta E = 1.0$ eV) operating in the constant analyser energy mode with a 15 eV pass energy setting the energy resolution at 1.0 eV. The Al Kα anode of the dual Al–Mg unmonochromated X-ray source (260 W, 57° mean incident angle) was employed in this study. Calibration of the analyser energy scale is performed acquiring AES and XPS spectra on a clean copper sheet of well referenced energies [4]. After a Shirley type background removal, experimental spectra recorded on such thin oxidized films can be decomposed into oxidized (film) and metallic (substrate) contributions

Table 2
Labeling of specimens according the oxidizing conditions

Condition	Specimen	O_2 Exposure time (h)	O_2 Pressure (mbar)	Main type of superficial oxide	Estimated thickness (oxide atomic monolayer)
Non-oxidized	DNO2	0	0	No oxide	–
Low oxidation	D0.5O2	0.5	20	Cr_2O_3	2–3
Medium oxidation	D4O2	4–8	20	$Fe_{1+x}Cr_{2-x}O_4$	5–6
Air-oxidized	DAO2	100	210	Fe_2O_3	11–12

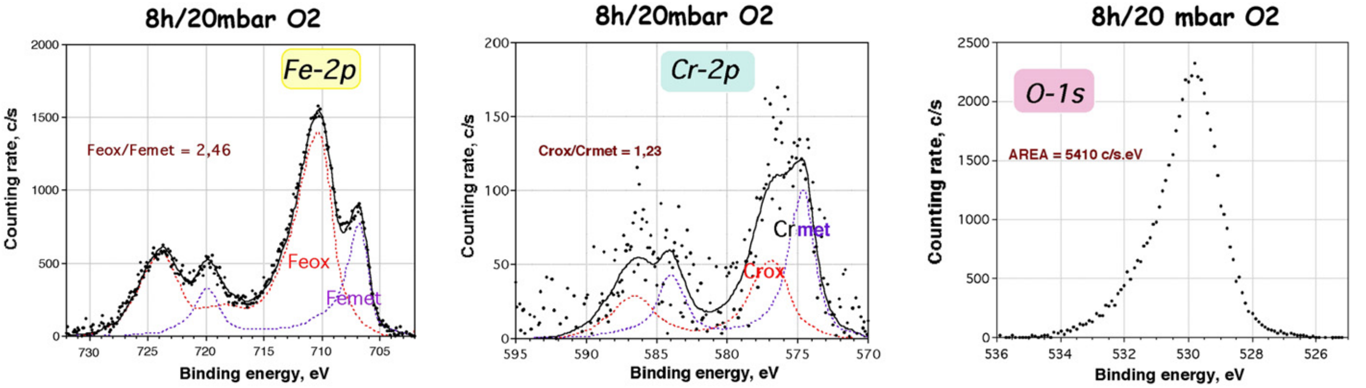

Fig. 3. Fe-2p, Cr-2p and O-1s XPS spectra recorded after 8 h oxidation at room temperature. Mox oxidized (film) and Met metallic (substrate) signal contributions in Fe and Cr XPS spectra are determined after a spectral decomposition using linear combinations of Fe, Fe_2O_3, 'FeO' and Cr, Cr_2O_3 reference spectra [7].

making linear combinations of Fe, Fe (II) and (III) oxides and Cr, Cr_2O_3 reference spectra with a minimization of their least square differences [5]. The approximate film thickness is expressed in monolayer equivalents deduced from known electron mean free data in metallic materials [6].

From the XPS analysis, it was established that the oxide film built after a short oxidation stage (<0.5 h – 20 mbar O_2) is mainly composed of Cr_2O_3. On the opposite, after a medium oxidation exposure (4–8 h – 20 mbar O_2), its surface is found mostly covered by an iron oxide, possibly of a spinel $Fe_{1+1}Cr_{2-x}O_4$ type (Fig. 3) [7]. This is in accordance with the wet or dry corrosion behavior of Fe–Cr alloy for which, during the fast initial oxidation step, the surface segregation of Cr induced by oxygen promotes the preferential oxidation of this element. During the later oxide growth, a faster and outward migration of Fe cations through the Cr_2O_3 film located at the alloy–oxide interface, contributes to build an iron external oxide film mostly composed by Fe_2O_3 [8]. So in the air oxidized condition, one finds an outer layer of Fe_2O_3. The film thickness is accordingly correlated to the exposure time.

4. SPT results

The load–displacement curves of the SPT performed at 250 °C and 300 °C of the different oxidation conditions are given in Fig. 4. Taking as reference the SPT curve of the air oxidized specimen (DAO2), the load-displacement curves of the other specimen (D4O2, D0.5O2, DNO2) are systematically below. The behaviors of the DNO2 specimens are very remarkable in their lower values of the yield point values. This is indicative of a strong LME effect occurring at low strain. Interestingly, there is also a tendency to measure decreasing load values (at a given displacement value) with decreasing the oxide layer thickness. The effect of oxide layer thickness appears to be correlated to the fracture energy values (see Table 3) calculated from the load-displacement integral. Indeed, the total energy for final fracture increases as a function of the oxide thickness. It indicates an effect on crack initiation and crack propagation linked with the oxide type. The fracture energy however is not a univocal indicator and must be complemented by a fractographic analysis which is the subject of the next section.

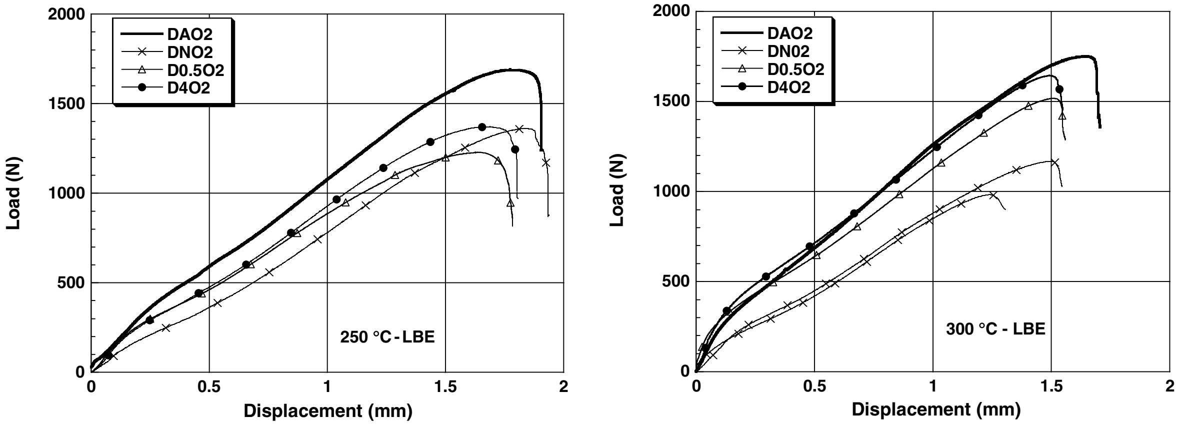

Fig. 4. SPT curves at 250 °C and 300 °C for different oxidation conditions (see Table 2 for labeling).

Table 3
Fracture energy evaluated from SPT curves according the oxidizing conditions and tests temperatures (see Table 2 for labeling)

Test temperature (°C)	DAO2 (J)	DNO2 (J)	D0.5O2 (J)	D4O2 (J)
250	1.91	1.44	1.34	1.46
300	1.79	0.87[a]	1.40	1.52

[a] The experiment was repeated twice, the result reported is the mean value.

5. SEM analysis

Due to the fact that the LBE layer is not very thick (of the order of a few micrometers at most), the SEM analysis were first performed on most samples with the remaining coating of PbBi and then after complete removal. This was accomplished by the selective dissolution of PbBi coating in a chemical composition composed of 1/3 ethanol, 1/3 acetic acid, 1/3 hydroxed water. This chemical solution is known not to affect fracture surfaces of steels.

Fig. 5 shows a SEM macro top view of the DNO2 (non-oxidized condition) sample after being tested at 300 °C (here PbBi has been removed). A lot of circular cracks can be seen. The SEM scans presented in Fig. 6 taken near the crack initiation site show a difference in the fracture modes as a function of the oxidizing condition. It can be seen that the DNO2 specimen (non-oxidized condition) exhibits a fully transgranular brittle fracture surface (Fig. 6(a)). On the other hand, a ductile fracture was observed in the DAO2 specimen (native oxide condition) without any sign of brittleness (Fig. 6(d)). However, the mechanical responses were not so much different in terms of curve shape as reported previ-

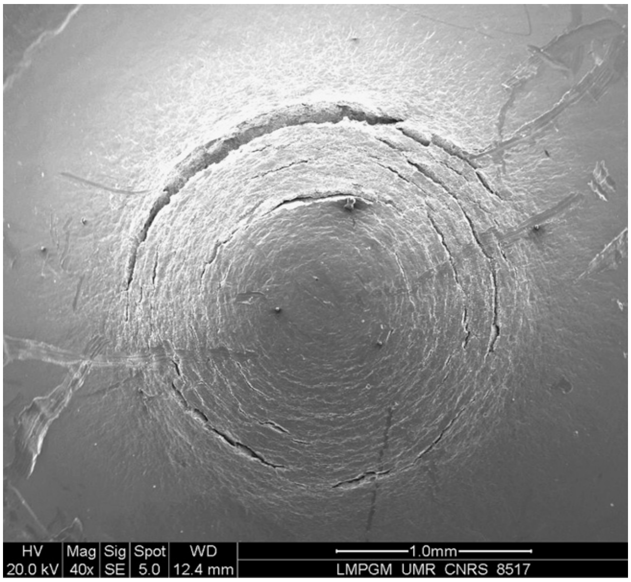

Fig. 5. Top view of the DNO2 (non-oxidized) specimen after fracture at 300 °C in contact with LBE.

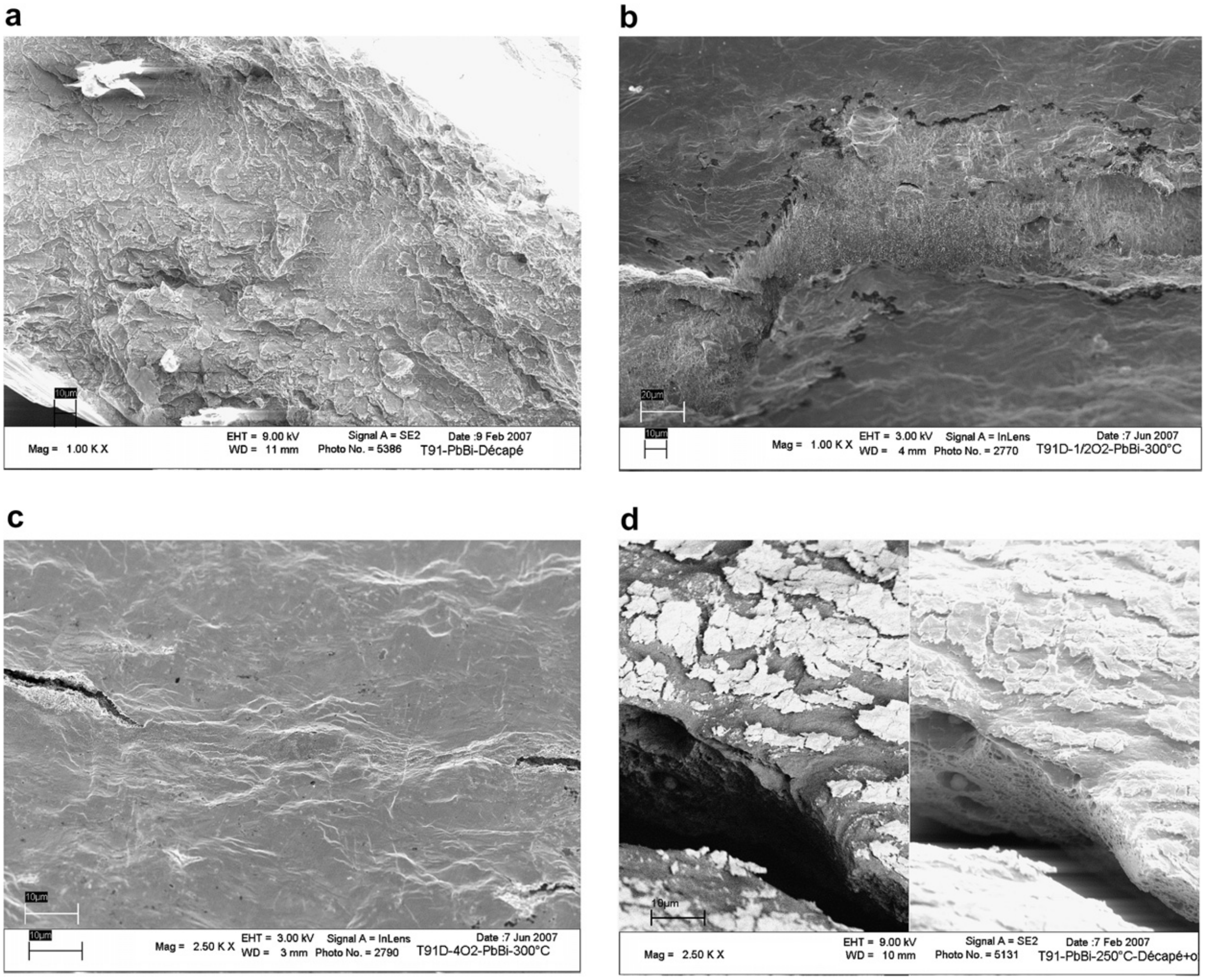

Fig. 6. SEM images of the fracture surface ((a), (b), (c) 300 °C; (d) 250 °C) (a) DNO2 (b) D0.5O2 (c) D4O2 and (d) DAO2 (see Table 2 for labeling).

ously [2]. For the two other samples, D0.5O2 and D4O2, intermediate situations were obtained. In the D0.5O2 specimen, (low oxidation condition) multiple cracking on the disc top did not occur. The fracture near the external surface looks fully ductile without any brittle fracture. Surprisingly, the D4O2 specimen (the medium oxidation condition) exhibits multiple cracking like as in the DNO2 specimen (the non-oxidized condition). The fracture surfaces near the external surface of most cracks were found to be of brittle transgranular type. In this case however, the brittle zone extended at most up to a few tens of microns. SEM views (not shown in the present paper) taken before PbBi dissolution with the Back Scattering Electron mode clearly show that PbBi is found on the brittle fracture surfaces overcoming the wetting barrier of the oxide. This clearly shows that in spite of the presence of the oxide, a brittle fracture promoted by the liquid PbBi alloy is possible and that not any type of oxide layer can guarantee a protection against LME. The small area concerned with the brittle fracture is most likely linked with the limited amount of PbBi deposited on the surface by the PVD technique. However, the size of the affected zone is large enough to be considered as being a definite proof that LME can occur in spite of the development of an already quite thick oxide.

6. Discussion: on the role of the oxide nature on LME cracking

One interesting fact is that the SPT experiment has been able to reproduce the effect of the liquid PbBi alloy in intimate contact with the T91 steel as shown previously with the tensile test [1]: combining intimate contact and plastic deformation, a brittle fracture can occur in the ductile T91 steel. The bi-axial stress state existing at the surface seems more damaging than a pure tensile component because the effect is very strong from the yield point. On the other hand, the native oxide is found as being totally protective against LME. This is an important point that demonstrates the suitability of the SPT technique for such studies.

Another interesting finding in this work is that the buildup of an oxide film on Fe–Cr alloys, supposed therefore, to avoid an intimate contact, is not necessarily protective against LME. Even in the case of an oxidized surface, LME can occur as exemplified with the medium oxidation condition in this work. The chemical composition of the oxide plays an important role on LME occurrence: an oxide type of dominantly Cr_2O_3 resulting from a short time exposure (low oxidation condition) seems to be protective. On the other hand, a medium exposure oxidation film containing iron oxides is possibly of a spinel type $Fe_{1+x}Cr_{2-x}O_4$. It is also known that during aging of a Fe–Cr alloy oxide film, the Fe^{2+} is converted to Fe^{3+} to progressively give Fe_2O_3 [7,8]. Therefore, these types of oxides evolve with time and a different wettability of the different iron-chromium oxides could explain the difference in fracture mode between the medium oxidation and the native oxide. Hydroxides formed on the native oxide or carbon contaminant could also be involved. If wetting is the key and single criterion for LME, these results suggest that wettability and diffusivity properties of these oxides should be investigated in detail separately. This will be left to a future work.

In conclusion, original experiments combining the SPT technique and XPS and/or Auger spectroscopy have been successfully carried out to study LME of the T91 steel. This was also one goal of this study. LME of the T91 is not only governed by an effective intimate contact between the liquid metal and the steel as often claimed. The chemical composition of the oxide, probably reflecting the wetting and diffusivity properties, on the steel surface could play an important role since Cr_2O_3 could be more protective than some mixed iron–chromium oxide films of the spinel type $Fe_{1+x}Cr_{2-x}O_4$.

Acknowledgements

The authors would like to acknowledge the financial support from the FP6 European program IP-EUROTRANS (contract N° FI6W-CT-2004-516520). Financial support from the French GDR GEDEPEON is also gratefully acknowledged.

References

[1] T. Auger, G. Lorang, Scr. Mater. 52 (12) (2005) 1323.
[2] I. Serre, J.B. Vogt, Nucl. Eng. Des. 237 (7) (2007) 677.
[3] F. Pons, J. Le Héricy, J.-P. Langeron, Surf. Sci. 66 (1979) 565.
[4] M.P. Seah, G.C. Smith, M.T. Anthony, Surf. Interf. Anal. 18 (1990) 293.
[5] F. Basile, J. Bergner, C. Bombart, B. Rondot, P. Le Guevel, G. Lorang, Surf. Interf. Anal. 30 (2000) 154.
[6] M.P. Seah, C.P. Hunt, Surf. Interf. Anal. 1 (1979) 2.
[7] J. R Lince, S. Didziulis, D.K. Shuh, T.D. Durbin, J.A. Yarmoff, Surf. Sci. 277 (1992) 43.
[8] M. Bouttemy, PhD Thesis of Paris XI University (Paris-Sud Orsay), October, 2006.